

Channel Modeling and Analysis for Molecular Motors in Nano-scale Communications

Youssef Chahibi^{*}
School of Electrical and Computer Engineering
Georgia Institute of Technology
Atlanta, USA

Ilangko Balasingham[†]
Department of Electronics and
Telecommunications
Norwegian University of Science and Technology
&
Intervention Center
Oslo University Hospital
&
Institute of Clinical Medicine
University of Oslo

ABSTRACT

Molecular motor communication (MMC) is a class of walkway based molecular communication, which is realized through motor proteins. In MMC, chemical energy is converted into the mechanical transport of molecules on cellular tracks named microtubules. In this paper, a channel propagation model of MMC nanonetworks is proposed, capturing the stochastic nature of molecular motors, transport bidirectionality, chemical energy conversion, and the topology of microtubules. Closed-form expressions of the probability of presence, delay, and attenuation are derived. The results are validated against Markov Chain Monte-Carlo simulations. Unlike diffusion-based and flow-based communication, MMC is active, low-delay, bidirectional, controllable, and can carry significantly large molecules. These characteristics make MMC an ideal candidate for realizing nanonetworks.

1. INTRODUCTION

Molecular motors are biological nanomachines that enable living organisms to perform efficient mechanical work, in-

^{*}Youssef Chahibi is with the Broadband Wireless Networking Laboratory at the Georgia Institute of Technology, School of Electrical and Computer Engineering. The work of Youssef Chahibi is conducted during his stay at the Biomedical Sensor Network Research Group at the Norwegian University of Science and Technology (NTNU), Institute of Mathematics and Electronics during 2014-2015. Email: youssef@ece.gatech.edu.

[†]Ilangko Balasingham is with the Biomedical Sensor Network Research Group at the Norwegian University of Science and Technology (NTNU), Institute of Mathematics and Electronics, the Intervention Center at the Oslo University Hospital, and the Institute of Clinical Medicine, University of Oslo. Email: ilangkob@iet.ntnu.no.

Permission to make digital or hard copies of all or part of this work for personal or classroom use is granted without fee provided that copies are not made or distributed for profit or commercial advantage and that copies bear this notice and the full citation on the first page. To copy otherwise, to republish, to post on servers or to redistribute to lists, requires prior specific permission and/or a fee.

NANOCOM'15, September 21 - 22, 2015, Boston, MA, USA
Copyright 2015 ACM 978-1-4503-3674-1/15/09 ...\$15.00.
<http://dx.doi.org/10.1145/2800795.2800813>.

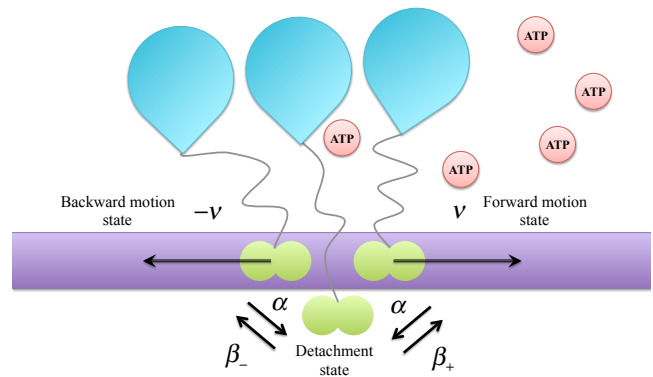


Figure 1: State representation of molecular motors motion.

cluding muscle contraction and the intracellular cargo transport [10]. In particular, kinesin and dynein are two important motor proteins enabling the intracellular cargo transport towards and away from the cell nucleus, respectively. They convert energy in the form of adenosine triphosphate (ATP) to transport large molecules inside a cell between different organelles and vesicles.

Molecular motor communication (MMC) is a type of walkway based molecular communication [1] mechanisms. MMC also underlies other walkway based molecular communication mechanisms such as chemotaxis by controlling the flagellum motor and neuron communication [6] by transporting large molecules along the axons of a neuron cell. Diffusion-based molecular communication [9] is not fast enough to transport molecules for distances larger than a μm . In addition, diffusion-based molecular communication cannot happen against the concentration gradient in the medium. Similarly, flow-based communication [2] cannot occur against the flow direction. MMC does not have this limitation. In fact, molecular motors can transport molecules in non-equilibrium mediums, regardless of the concentration gradient, by using chemical energy (e.g. in the form of ATP) to produce a mechanical movement in a similar way to an auto engine. The ability to control the motion of molecular motors using molecular switches [3] makes MMC a promising solution to realize nanonetworks.

Unlike macro-scale motors, molecular motors are highly stochastic in nature. MMC has been conceptually considered as a molecular communication mechanism in [11]. In [7], MMC using microtubule transport over kinesin-coated surfaces has been simulated based on a mobility model that assumes a drift velocity and a Brownian motion diffusivity of the microtubule calculated empirically from experimental observations. In reality, the drift velocity and diffusivity are highly coupled. Moreover, molecular motors often detach from their track and diffuse freely along the track. In this paper, an analytical model and performance analysis of MMC channel propagation is derived based on the mobility parameters (backward motion, forward motion, and detachment) of the molecular motor protein (kinesin and dynein) moving along a microtubule cf. Fig. 1). The channel delay and attenuation over a microtubule are expressed as closed-form expressions of the propagation distance and the mobility parameters. In addition, the channel propagation model considers different boundary conditions at the extremity of the MMC nanonetwork such as absorbing and reflecting ends. The results are validated by comparison with Markov Chain Monte-Carlo simulations [4].

Molecular motors are involved in several diseases and therapeutic methods. In fact, several brain conditions such as Parkinson's and Alzheimer are associated to jamming in microtubules. Molecular motors signaling is important for finding methods to trigger the death of diseased cells. The study of molecular motors has intrigued the scientific community, especially that they are difficult to observe, and the more advances in cell imaging develop, the more complex the mechanisms underlying molecular motors are revealed to be [5].

The paper is organized as follows. In Section. 2, the channel model based on the kinetics of molecular motor transport is presented. In Section. 3, the closed-form expressions of delay and attenuation are derived. In Section. 4, numerical results stemming from the channel model and the expressions of delay and attenuation are presented and discussed. Finally, Section 5 concludes the paper.

2. PROPAGATION CHANNEL MODEL

In this section, the propagation channel modeling is derived by describing the elements of the molecular communication abstraction of molecular motor nanonetworks.

2.1 System Abstraction

The nanonetworks abstraction of molecular motors models the network of microtubules (cytoskeleton) as a MC network composed of the following elements:

- *MC transmitter* (cargo production) which corresponds the location where the cargo transported by the molecular motor is produced and loaded into a kinesin or dynein protein. The location can be an organelle, a vesicle, or a the nucleus of the cell. The direction of the motion is determined by the transporting motor protein (kinesin or dynein).
- *MC links* (microtubules) which are the molecular tracks where the motor protein are traveling. Typically, their topology is star-shaped, and can span distances of the order of the μm .

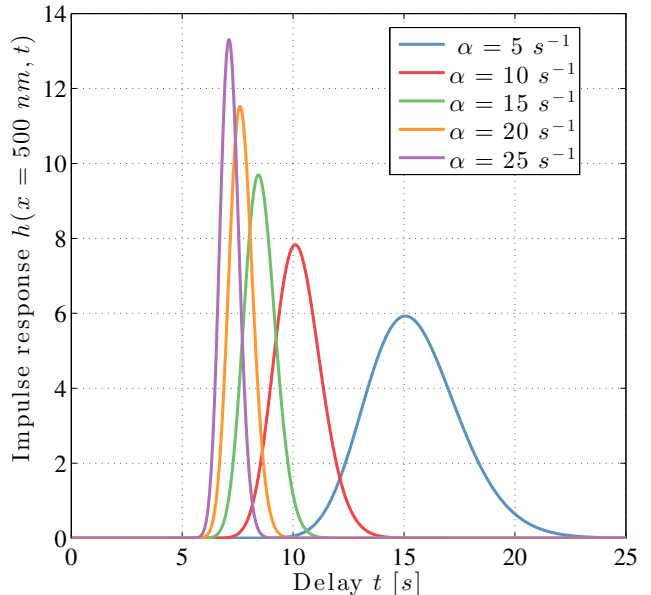


Figure 2: Probability of presence of a molecular motor channel for various detachment rates α .

- *MC signal* (cargo) The molecular motor can transport large molecules ten-fold faster than diffusion alone. The cargo can encapsulate an MC signal, for example, as a sequence of amino-acids.
- *MC receiver* (cargo detection) which corresponds to the location where the cargo is delivered and detected by another part of the cell, such as a vesicle, organelle, or nucleus. The reception can be either by detection or by consumption of the cargo.

The channel model is based on the experimental observations regarding the biophysics of protein transport inside the cell. It has been observed in [8], that molecular motors undergo the stochastic transitions between different motion states, namely the backward motion state, the detachment state, and the forward motion state with different rates β_- , α , and β_+ , respectively. As shown in Figure 1, the molecular motor moves with a speed $-\nu$ in the backward motion state, with a speed 0 at the detachment state, and with a speed ν at the forward motion state. The speed ν is a function of the chemical energy as follows [8]

$$\nu = \frac{\nu_{max} c_{ATP}}{c_{ATP} + K_\nu}, \quad (1)$$

where ν_{max} is the maximum speed, and K_ν is the saturation constant of ATP conversion, and c_{ATP} is the ATP concentration.

2.2 Link Models

Using the Fokker-Planck reduction of linear reaction-hyperbolic equations, we can find that the probability of presence $h(x, t)$ of a molecular motor is governed by the following equation

$$\frac{\partial h(x, t)}{\partial t} = V \frac{\partial h(x, t)}{\partial x} + D \frac{\partial^2 h(x, t)}{\partial x^2}, \quad (2)$$

where x is the spatial coordinate and t is the time variable.

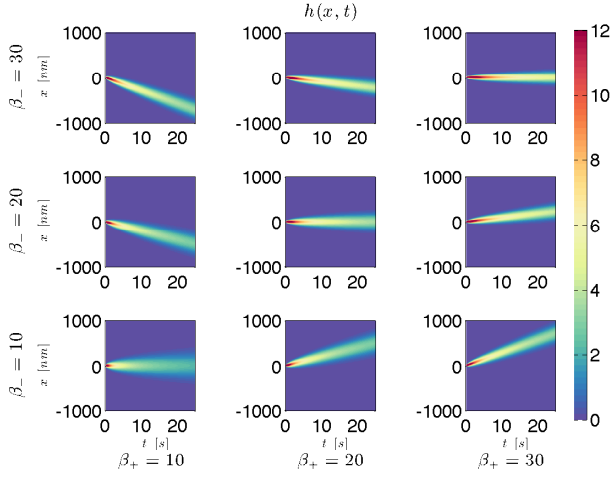


Figure 3: Influence of the backward and forward motion rates on the spatial and temporal distribution of molecular motors.

V is the drift term, expressed as

$$V = \frac{1}{\gamma} \left(\frac{1}{b_-} - \frac{1}{b_+} \right). \quad (3)$$

D is the diffusion term, expressed as

$$D = \epsilon \left[\frac{(1-V)^2}{\gamma b_-^2} + \frac{(1+V)^2}{\gamma b_+^2} \right], \quad (4)$$

with the transition rates given by

$$\begin{cases} b_+ = \eta \beta_+, \\ b_- = \eta \beta_-, \\ a = \eta \alpha. \end{cases} \quad (5)$$

The normalization variable γ and the non-dimensionalizing coefficient is η as follows

$$\begin{cases} \gamma = \frac{1}{b_+} + \frac{1}{b_-} + \frac{1}{a}, \\ \eta = \frac{\epsilon l}{v}, \end{cases} \quad (6)$$

where $\epsilon \ll 1$ and l is the characteristic size of the target area. The equations (3) and (4) show the coupling between the drift and the diffusion terms through the transitions rates of the molecular motor motion. This coupling is shown in Figure 3 where the probability of presence $h(x, t)$ is calculated for various values of the backward and forward motion rates, and in Figure 2, where it is calculated for different values of the detachment rate. Molecular motor tracks are interconnected as a network and can be terminated with open ends, reflecting ends, and absorbing ends as shown in Figure 4. We solve (2) for these different boundary conditions, by finding the probability of presences $h_O(x, t)$, $h_A(x, t)$, and $h_R(x, t)$, respectively, as follows:

- *Open end channel:*

$$h_O(x, t) = \frac{e^{-\frac{x^2}{4Dt} + \frac{V}{2D}(x-Vt)}}{\sqrt{4\pi Dt}} \quad (7)$$

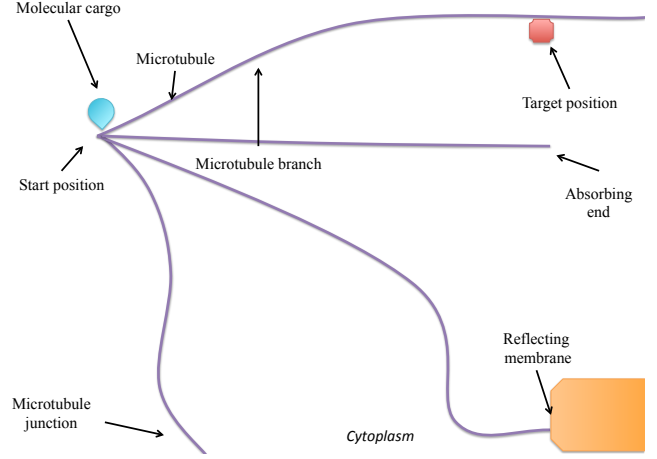


Figure 4: Molecular motors traveling in a network of microtubules.

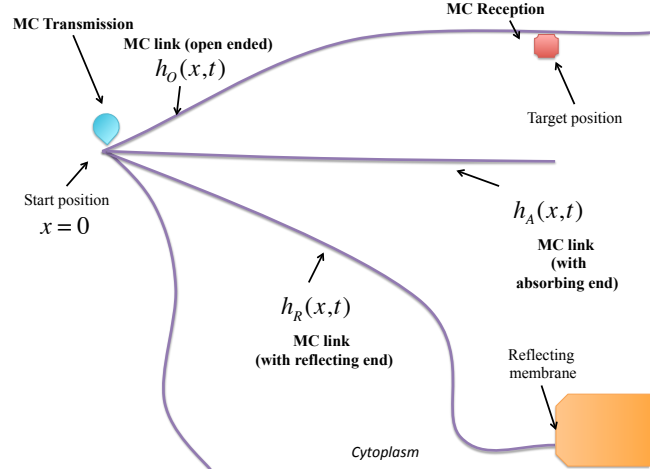


Figure 5: Nanonetworks abstraction of molecular motors propagation.

- *Absorbing end channel:*

$$h_A(x, t) = \left(\frac{e^{-\frac{x^2}{4Dt}}}{\sqrt{4\pi Dt}} - \frac{e^{-\frac{(2x_A-x)^2}{4Dt}}}{\sqrt{4\pi Dt}} \right) e^{\frac{V}{2D}(x-Vt)}, \quad (8)$$

with x_A the coordinate of the absorbing end.

- *Reflecting end channel:*

$$h_R(x, t) = \left(\frac{e^{-\frac{x^2}{4Dt}}}{\sqrt{4\pi Dt}} + \frac{e^{-\frac{(2x_R-x)^2}{4Dt}}}{\sqrt{4\pi Dt}} \right) e^{\frac{V}{2D}(x-Vt)}, \quad (9)$$

with x_R the coordinate of the reflecting end.

3. PERFORMANCE ANALYSIS

In this section, the delay and attenuation of the MMC are derived as a closed-form expression of the parameters of the molecular motor mobility and the propagation distance.

Table 1: Numerical values of the molecular motor model.

Parameter	Value
Forward motion rate β_+	10 s^{-1}
Reverse motion rate β_-	100 s^{-1}
Detachment rate α	1 s^{-1}
Absorption rate κ	0.05 s^{-1}
Speed ν_{max}	$0.1 \mu\text{ms}^{-1}$
ATP concentration c_{ATP}	$40 \mu\text{M}$
ATP saturation constant K_ν	$79.23 \mu\text{M}$
Receiver length l	$1 \mu\text{m}$
Number of molecular motors N_m	30,000
Spatial averaging distance dx	0.045 nm
Non-dimensionalizing coefficient ϵ	0.1

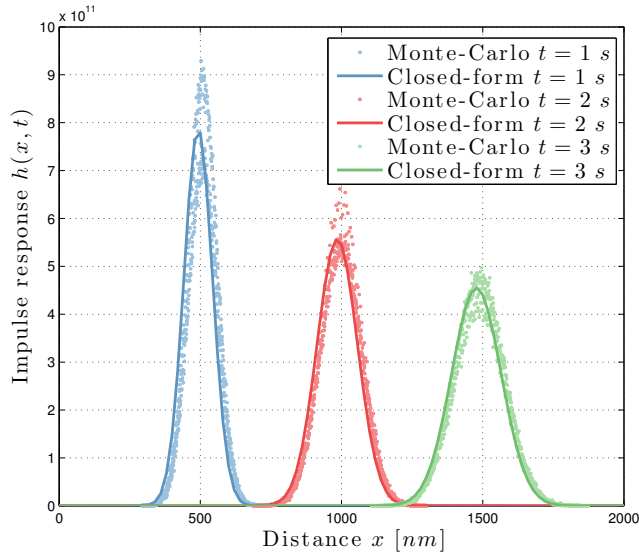


Figure 6: Comparison between the closed-form channel probability of presence expression and Markov chain Monte-Carlo simulations of the molecular motors motion.

3.1 Delay

The delay is defined as the time required by a molecular motor to reach its peak probability of presence in a coordinate x , as follows:

$$\tau(x) = \arg \max_t \{h(x, t)\}. \quad (10)$$

Based on (7), by taking the first derivation of $h(x, t)$ equal to zero, we find that the delay is expressed as follows:

$$\tau(x) = \frac{l}{\nu} \frac{\sqrt{D^2 + V^2 x^2} - D}{V^2}, \quad (11)$$

where l is the characteristic length of the molecular motor motion and ν is the speed of the molecular motor in forward motion. Due to the linear nature of the Fokker-Planck equation of MMC, the delay for a cascade of links can be calculated by the sum of the delays for each link.

3.2 Attenuation

The attenuation is defined as the peak probability of presence in the dB scale as follows:

$$A(x) = \max_t \{10 \log_{10} (h(x, t))\}. \quad (12)$$

Based on (7) and (11), we find that the attenuation is expressed as follows:

$$A(x) = 10 \log_{10} \left(\frac{V}{D} \frac{\exp \frac{\frac{Vx}{D} - \sqrt{1 + (\frac{Vx}{D})^2}}{2}}{\sqrt{4\pi \left(\sqrt{1 + (\frac{Vx}{D})^2} - 1 \right)}} \right). \quad (13)$$

Therefore, we have

$$A(x) = 10 \log_{10} \left(\frac{V}{D} \right) - 5 \log_{10} \left(\sqrt{1 + \left(\frac{Vx}{D} \right)^2} - 1 \right) + \frac{5}{\ln(10)} \left(\frac{Vx}{D} - \sqrt{1 + \left(\frac{Vx}{D} \right)^2} \right) - 5 \log_{10} (4\pi). \quad (14)$$

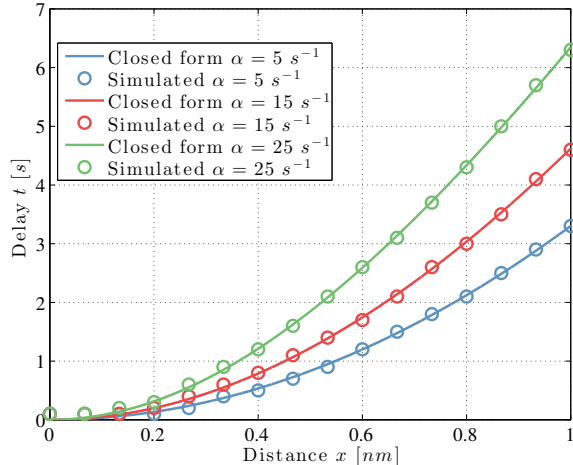
Due to the linear nature of the Fokker-Planck equation of MMC, the attenuation for a cascade of links can be calculated by the sum of the attenuations for each link. Also, we notice that a critical parameter of the attenuation is the ratio between the drift term and the diffusion term. To the best of our knowledge, this is the first work to provide an expression of delay and attenuation for molecular motor transport.

4. NUMERICAL RESULTS

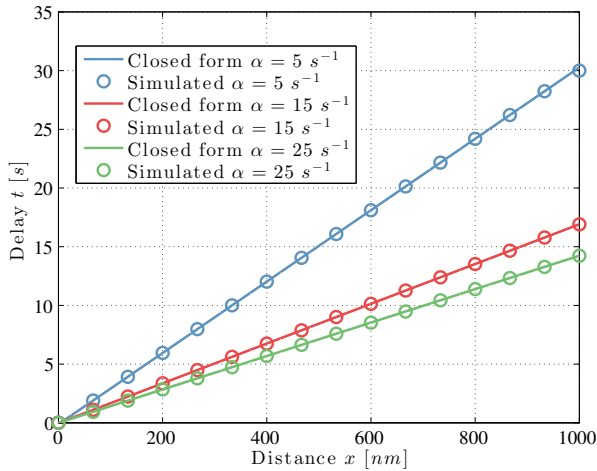
4.1 Monte-Carlo Simulation

Figure 6 compares the closed-form MMC probability of presence $h(x, t)$ with the histogram of the position of a molecular motor. The simulation parameters are listed in Table 1. The simulation environment consisted is based on the Markov Chain Monte-Carlo [4] method, where a number of molecular motors N_m is placed at the initial coordinate $x = 0$, and the motion of each molecular motor is dictated by a coin toss according to the transition diagram shown in Figure 8. Depending on this random outcome, the molecular motor either moves backward by a distance $-\nu dt$, forward by a distance νdt , or remains in a still position, where dt is the time increment of the simulation. The coin tossing is repeated until the end of the desired simulation time T is attained.

Finally, the probability of presence is estimated by evaluating the histogram of the positions of the N_m molecular motors, with a spatial averaging distance dx , and compared with the analytical solution of the Fokker-Planck equation. The closed-form and simulated probabilities of presence match favorably. We notice that contrary to diffusion transport, the noise, defined as the variance of the position of the molecular motors, seems to reduce as the distance increases, and that the noise remains very high compared with the high number of molecular motors N_m on which the results have been ensemble averaged.



(a) Small-scale regime ($x < 1 \text{ nm}$).



(b) Large-scale regime ($x > 1 \text{ nm}$).

Figure 7: Molecular motor channel delay for different detachment rates α exhibiting a small-scale regime for ($x < 1 \text{ nm}$) and a large-scale regime for ($x > 1 \text{ nm}$).

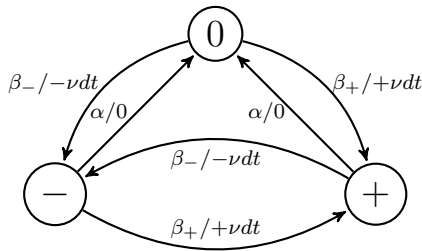


Figure 8: Markov-chain representation of the molecular motor motion.

4.2 Delay

Figure 7 shows the delay of an MMC channel within a small-scale ($x < 1 \text{ nm}$) or a large-scale ($x > 1 \text{ nm}$). The figures show that there are two regimes for the delay-distance relationships. First, in the small-scale, the delay follows a non-linear relationship with respect to the distance. Second, in the long range the delay becomes quickly a linear expression of the distance. This is different from diffusion where the delay increases as the square of the distance, showing the advantages of MMC over other types of molecular communication mechanisms.

The numerical results match with the experimental measurements of molecular motor speeds in the order of a hundred nm per second. Although this speed may appear low, it is very large compared with the size of the molecular motor and with diffusion-based transport.

4.3 Attenuation

Figure 9 shows that the attenuation of a MMC channel is very high within a few nm , which suggests that the molecular motor channel is highly noise in nature, however, in contrast with diffusion Brownian motion, the motion is directed.

In the dB scale, the attenuation is very high from 0 to 1 nm (from 0 to -50), but for the longer scale, from 1 nm to 10 nm , the attenuation does not vary dramatically (less than 10 dB difference). Whereas the delay is highly dependent on the drift term V and less on the diffusion term D , the attenuation depends only on the ratio of the two V/D and the propagation distance x . The detachment rate α does not significantly affect the attenuation, compared with its important influence on the MMC delay.

5. CONCLUSION

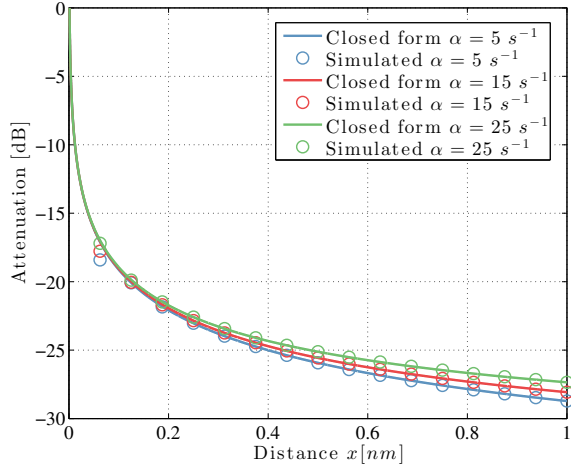
A method to obtain the propagation channel model of an MC-MM network was derived, including closed-form expressions of probability of presence for different topologies. The modeling enables to find the closed-form expression of the delay and attenuation. It was observed that the delay in the case of diffusion increases with the square of the propagation distance, whereas for active transport, the delay increases linearly with the propagation distance.

We propose for future work to develop realistic models of bifurcations and junctions to model molecular transport in dendritic trees. This channel propagation model can enable the study of other aspects of molecular motors such as energy consumption, noise, information-theoretical capacity, and modulation schemes. Molecular motor communication outperforms other classes of molecular communication such as diffusion-based and flow-based communication, which makes it a suitable candidate for designing bio-inspired nanonetworks.

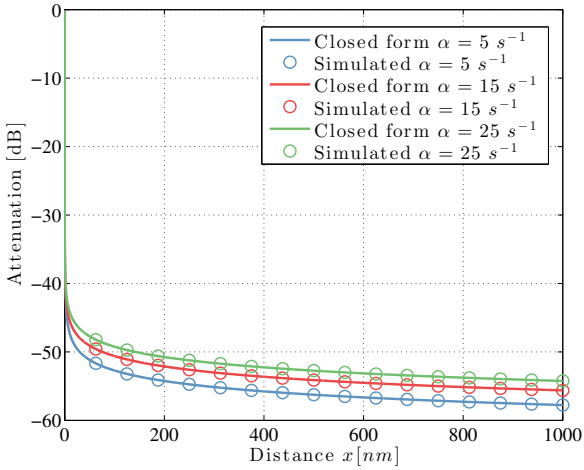
6. ACKNOWLEDGEMENTS

The authors would like to thank Prof. Ian F. Akyildiz for his constructive criticism which helped to improve the quality of the paper and the referees for their excellent and constructive feedback. This material is based upon work supported by the Norwegian Research Council as a part of the MELODY project.

7. REFERENCES



(a) Small-scale behavior.



(b) Long-scale behavior.

Figure 9: Molecular motor channel attenuation for different detachment rates α for small-scale ($x < 1 \text{ nm}$) and large-scale ($x > 1 \text{ nm}$).

- [1] I. F. Akyildiz, F. Brunetti, and C. Blázquez. Nanonetworks: A new communication paradigm. *Computer Networks*, 52(12):2260–2279, 2008.
- [2] Y. Chahibi, I. Akyildiz, S. Balasubramaniam, and Y. Koucheryavy. Molecular communication modeling of antibody-mediated drug delivery systems. *IEEE Transactions on Biomedical Engineering*, PP(99):1–1, 2015.
- [3] J. C. Cochran, Y. C. Zhao, D. E. Wilcox, and F. J. Kull. A metal switch for controlling the activity of molecular motor proteins. *Nature structural & molecular biology*, 19(1):122–127, 2012.
- [4] W. R. Gilks. *Markov chain monte carlo*. Wiley Online Library, 2005.
- [5] W. O. Hancock. Bidirectional cargo transport: moving beyond tug of war. *Nature Reviews Molecular Cell Biology*, 15(9):615–628, 2014.
- [6] F. Mesiti and I. Balasingham. Nanomachine-to-neuron communication interfaces for neuronal stimulation at nanoscale. *IEEE Journal on Selected Areas in Communications*, 31(12):695–704, 2013.
- [7] M. J. Moore, T. Suda, and K. Oiwa. Molecular communication: modeling noise effects on information rate. *IEEE Transactions on NanoBioscience*, 8(2):169–180, 2009.
- [8] J. M. Newby and P. C. Bressloff. Quasi-steady state reduction of molecular motor-based models of directed intermittent search. *Bulletin of mathematical biology*, 72(7):1840–1866, 2010.
- [9] M. Pierobon and I. F. Akyildiz. Capacity of a diffusion-based molecular communication system with channel memory and molecular noise. *IEEE Transactions on Information Theory*, 59(2):942–954, 2013.
- [10] M. Schliwa. *Molecular motors*. Springer, 2006.
- [11] T. Suda, M. Moore, T. Nakano, R. Egashira, A. Enomoto, S. Hiyama, and Y. Moritani. Exploratory research on molecular communication between nanomachines. In *Genetic and Evolutionary Computation Conference (GECCO), Late Breaking Papers*, pages 25–29, 2005.